



## Solution-processed p-doped hole-transport layer and its application in organic light-emitting diodes

Xinwen Zhang<sup>a</sup>, Zhaoxin Wu<sup>a,\*</sup>, Dawei Wang<sup>a</sup>, Dongdong Wang<sup>b</sup>, Runlin He<sup>c</sup>, Xun Hou<sup>a</sup>

<sup>a</sup> Key Laboratory of Photonics Technology for Information, Key Laboratory for Physical Electronics and Devices of the Ministry of Education, School of Electronic and Information Engineering, Xi'an Jiaotong University, Xi'an 710049, PR China

<sup>b</sup> School of Science, Xi'an Jiaotong University, Xi'an 710049, PR China

<sup>c</sup> Firefly Lighting Co., Ltd., Xiamen 361010, PR China

### ARTICLE INFO

#### Article history:

Received 12 January 2010

Received in revised form 22 January 2010

Accepted 22 January 2010

Available online 1 February 2010

#### Keywords:

Organic light-emitting diodes

Solution-processed

p-Doped hole-transport layer

Stability

### ABSTRACT

We investigate p-type doping poly(9-vinylcarbazole) (PVK) hole-transport layer (HTL) with tetrafluoro-tetracyano-quinodimethane introduced via cosolution. We found that the performances of devices with doped HTLs are significantly improved. The efficiency and lifetime of the p-doped device are 2.3 and 3.7 times as large as that of the control device with pure PVK as a HTL. Furthermore, the turn-on voltage of the device is reduced from 9.5 to 3.6 V by using a p-doped HTL. These improved properties are attributed to the formation of the charge-transfer complex in the HTL, which increases hole injection and conductivity of p-doped films considerably.

© 2010 Elsevier B.V. All rights reserved.

### 1. Introduction

Organic light-emitting diodes (OLEDs) have attracted much attention because of their potential application in flat panel displays and solid state lighting devices [1,2]. To achieve lower driving voltages and higher power efficiency, efficient charge injection from the electrodes into the charge transport layers (CTLs) and the subsequent transporting in these layers are of crucial importance for display applications [3–5]. Since the injection requires charge carriers to overcome the energy barriers in the electrode/CTL interfaces [6], a high forward bias is usually needed to drive the device. To achieve lower operating voltage, one need to reduce Ohmic losses of charge injection at the interface, and increase charge transporting ability inside the film. Several methods have been introduced to increase the efficiency of hole injection in OLEDs. These methods include increasing the work function of indium–tin oxide (ITO) by special surface treatments [7–9], and introducing a hole injection layer or an anode buffer layer [10–12].

The p-doping hole-transport layer (HTL) has drawn a lot of attention in recent years because of its ability to enhance hole injection and thus achieve lower driving voltages in OLEDs [4–6,13–16]. For small molecule materials, the p-doping of HTL is

typically realized by co-evaporating the hole-transporting materials with a strong electron acceptor like tetrafluoro-tetracyano-quinodimethane (F4-TCNQ) [4], molybdenum oxide ( $\text{MoO}_3$ ) [5], copper iodide (CuI) [13], tungsten oxide ( $\text{WO}_3$ ) [14], rhenium oxide ( $\text{ReO}_3$ ) [15] and vanadium oxide ( $\text{V}_2\text{O}_5$ ) [16]. However, it is difficult to control precisely the formation of the doped film in the vapor deposition process. As an alternative approach, the solution-based processing method is expected to reduce manufacture cost and avoid the complexity of co-deposition process. Solution-processed polymer semiconducting layers, which are p-doped, have been developed by spin-coating co-solutions on the ITO substrates [17–24]. It has been reported that, the doped polymer HTLs show considerable reduction in driving voltage compared to a conventional device and greatly contribute to the enhancement of the device stability [22].

In this letter, we investigate how p-doping can significantly improve the performance of devices employing poly(9-vinylcarbazole) (PVK) as the HTL. As a hole-transport material, PVK has been widely used either in two-layer [25,26] or multilayer devices [27,28]. However, these devices had high turn-on voltages and low efficiency because of the large hole injection barrier at ITO/PVK (about 1.0 eV) and lower mobility of PVK [29]. As studies show that the conductivity of PVK thin film can be increased by doping [30,31], we present a study of the hole injection and conductivity of F4-TCNQ-doped PVK. In particular, we investigate the effect of p-doped HTLs on the performances of OLEDs. Using absorption spectra of the doped film, we have found that, charge-transfer (CT)

\* Corresponding author. Tel.: +86 29 82664867; fax: +86 29 82664867.  
E-mail address: [zhaoxinwu@mail.xjtu.edu.cn](mailto:zhaoxinwu@mail.xjtu.edu.cn) (Z. Wu).

complex forms between F4-TCNQ and PVK, and this CT complex significantly enhances the hole-current in a F4-TCNQ-doped PVK layer. The current efficiency, the turn-on voltage and operational stability are significantly improved in the devices using F4-TCNQ-doped PVK layers.

## 2. Experimental

The devices have the structure of ITO/PVK:*x* wt.% F4-TCNQ (50 nm)/NPB (10 nm)/Alq<sub>3</sub> (60 nm)/LiF (0.5 nm)/Al (100 nm). In the devices, F4-TCNQ-doped PVK was used as the p-doped HTL. *N,N'*-di(naphth-1-yl)-*N,N'*-diphenyl-benzidine (NPB) was the interlayer, and tris(8-hydroxyquinolino) aluminum (Alq<sub>3</sub>) served as the emitting layer (EML) as well as the electron-transport layer while LiF/Al was used as a bilayer cathode. In the experiment, F4-TCNQ (Aldrich) was dissolved in 1,2-dichloroethane and PVK (*M<sub>w</sub>*: 1 100 000, Aldrich) was dissolved in chlorobenzene, respectively. The two solutions were then mixed at different ratios to achieve 2, 5, 10, and 15 wt.% (dopant to host weight ratio) doping concentrations. The p-doped HTL was spin coated onto the pre-cleaned ITO substrate, and then the samples were dried in an oven for 1 h at 80 °C. The thickness of these spin-coated films was approximately 50 nm. Subsequently, NPB (10 nm) and Alq<sub>3</sub> (60 nm) were deposited by thermal evaporation in a vacuum chamber at a pressure of  $5 \times 10^{-4}$  Pa, while LiF (0.5 nm) and Al (100 nm) were fabricated by thermal evaporation in vacuum without the break. The deposition rates of organic layer, LiF and Al were 0.1–0.2, 0.02–0.04, and 0.3–0.5 nm/s, respectively. Following the same procedure as the above, hole-only devices were also fabricated. The structures of the hole-only devices are ITO/PVK:*x* wt.% F4-TCNQ (100 nm)/NPB (10 nm)/Al (100 nm) (bulk doping) and ITO/PVK:*x* wt.% F4-TCNQ (10 nm)/NPB (100 nm)/Al (100 nm) (interface doping). The absorption spectra of the PVK and F4-TCNQ-doped PVK films were recorded by a spectrophotometer (U-3010 Hitachi Inc). The surface morphology of the ITO and the organic thin films were examined by an atomic force microscope (AFM). The electroluminescence characteristics of the devices were measured by a Keithley 2602. The operational stability measurements of the encapsulated devices were performed using a constant DC current. All measurements were carried out at room temperature under ambient conditions.

## 3. Results and discussion

Fig. 1 shows the absorption spectra of PVK and F4-TCNQ-doped PVK films at various doping concentrations. A pure PVK thin film shows no absorption above 400 nm, while the doped PVK thin films show an additional absorption band around 650 nm. This

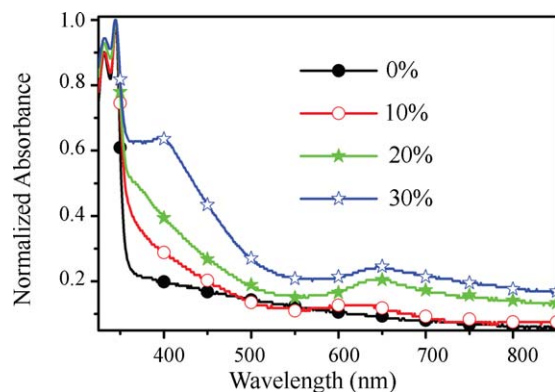


Fig. 1. Absorption spectra of pure and F4-TCNQ-doped (10, 20, and 30 wt.%) PVK thin films, normalized to the PVK absorption at ~345 nm.

new peak at 650 nm is a strong sign indicating that CT complex has formed in the HTL. This formation of the CT complex is mainly due to the jumping of an electron from a donor molecule (the PVK) to an electron acceptor molecule (the F4-TCNQ) [4,5,13–15]. Here, it is interesting to note that for this particular CT complex of PVK and F4-TCNQ, a new transition peak at about 1.9 eV (650 nm) appears, and this peak is stable with increasing concentration of F4-TCNQ. Similar phenomena have been observed in the absorption spectra of thin films doped with small molecules (doped with F4-TCNQ [4], MoO<sub>3</sub> [5], CuI [13], WO<sub>3</sub> [14], and ReO<sub>3</sub> [15]) and conjugated polymers (such as I<sub>2</sub>-doped MEH-PPV [17], and F4-TCNQ-doped poly(3-hexylthiophene) [19]). These reports indicate that the CT complex is an important phenomena that is essential for understanding the characteristics of doped organic materials [19].

Using our devices, we investigated the effects of the CT complex composed of F4-TCNQ-doped PVK on the hole injection and transport. Fig. 2(a) shows the current density–voltage characteristics of the doped hole-only devices, which have the structure ITO/PVK:*x* wt.% F4-TCNQ (100 nm)/NPB (10 nm)/Al (100 nm). They are fabricated with PVK and doped PVK with various weight percentage concentrations of F4-TCNQ. It is clear that, at the same voltage, the hole-current increases significantly with the concentration of F4-TCNQ doping. Table 1 shows the required voltages to achieve 20 and 100 mA/cm<sup>2</sup> current density in hole-only devices. We see that, the voltage to obtain a current of 20 mA/cm<sup>2</sup> is decreased from 18.5 to 7.5 V when the doping concentration is increased from 0 to 15 wt.%. Similar result is also obtained for a current of 100 mA/cm<sup>2</sup>. Doping with F4-TCNQ has apparently lead to significant increase in hole-current in the hole-only devices. The device with 15 wt.% F4-TCNQ-doped PVK has a hole-current that is more than three orders of magnitude larger than that of the device

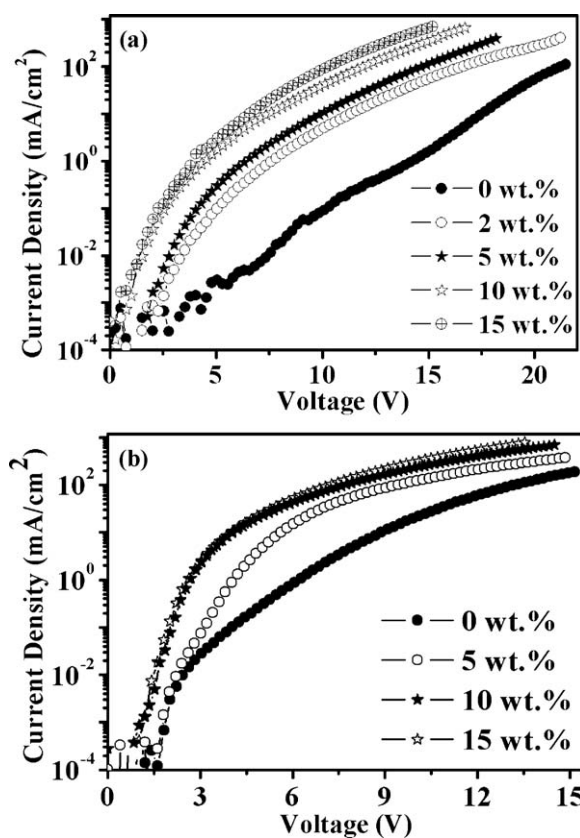


Fig. 2. The current density–voltage characteristics of the hole-only devices at different F4-TCNQ concentrations in PVK: (a) ITO/PVK:*x* wt.% F4-TCNQ (100 nm)/NPB (10 nm)/Al (100 nm) and (b) ITO/PVK:*x* wt.% F4-TCNQ (10 nm)/NPB (100 nm)/Al (100 nm).

**Table 1**Voltage of bulk-doped hole-only devices at current densities of 20 and 100 mA/cm<sup>2</sup>.

Hole-only devices	Voltage (V) at 20 mA/cm <sup>2</sup>	Voltage (V) at 100 mA/cm <sup>2</sup>
0 wt.%	18.5	21.2
2 wt.%	12.7	16.6
5 wt.%	11.3	14.7
10 wt.%	8.7	11.0
15 wt.%	7.5	10.3

without doping. We attribute this significant increase to two effects that are induced by the formation of CT complex: the enhanced hole injection through the ITO/HTL interface and the increased electrical conductivity in the doped layer. To distinguish the two effects and estimate their separate contributions to the enhanced current, we fabricated another hole-only device with a ~10 nm doped PVK layer. The structure of the hole-only device is ITO/PVK:*x* wt.% F4-TCNQ (10 nm)/NPB (100 nm)/Al (100 nm). Comparing to the other device (100 nm F4-TCNQ-doped PVK), we can consider the 10 nm F4-TCNQ-doped PVK as an interface injection layer with no significant influence on hole-transportation in the device. In fact, the 100 nm NPB is the HTL in this device. Fig. 2(b) shows the current density as a function of applied voltage of the hole-only devices with 0, 5, 10 and 15 wt.% F4-TCNQ-doped PVK interface layers. The devices with a F4-TCNQ-doped interface layer exhibit higher hole-current than that of the device using pure PVK as the interface layer. Under 4 V driving voltage, the hole-current density is increased from 0.1 mA/cm<sup>2</sup> for the without doped device to 10 mA/cm<sup>2</sup> for the 15 wt.% doped device, which indicates that the p-doped interface layers significantly enhance the hole injection.

From above results, we can conclude that the p-doped polymer is achieved by the simple co-solutions of F4-TCNQ and PVK. p-Doping occurs via electron transfer from the HOMO level of the PVK to the LUMO level of the F4-TCNQ. This leads to a shift of the Fermi level toward the PVK HOMO level, which offers a lower barrier to current injection compared to the pure PVK device [18,19]. The improvement of hole-current is caused not only by the increase in film conductivity, but also by the decrease in interface injection barrier of ITO/p-doped PVK due to the formation of CT complex [19]. To understand this enhanced injection, the energy diagram of the devices was presented in Fig. 3. In the device with the PVK layer, hole injection ability depends apparently on the

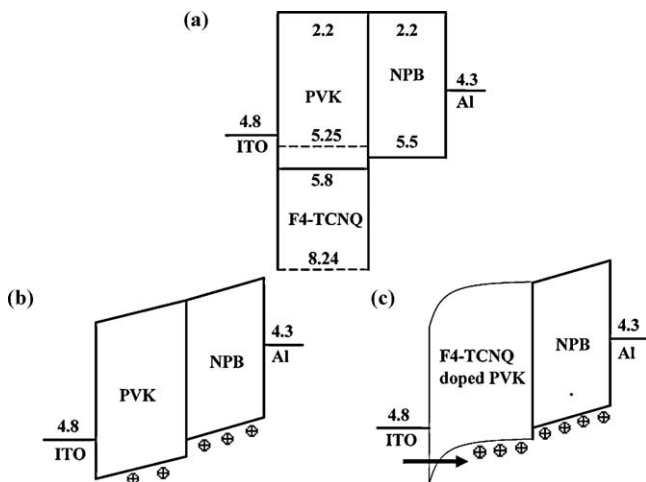


**Fig. 3.** (a) Schematic energy-level diagram of hole-only device; (b) sketch showing the energy barrier of hole injection in the device with pure PVK layer; (c) sketch showing the energy barrier of hole injection in the device with p-doped PVK layer.

energy barrier between anode (ITO) Fermi level and the HOMO level of the PVK layer, therefore the current is injection-limited due to the big hole injection barrier (about 1 eV) at the ITO/PVK interface (Fig. 3(b)). However, in the p-doped PVK layer, because the Fermi level is close to the PVK HOMO level, the CT complex causes a space charge region near the interface of ITO/p-doped PVK. With increasing doping, the width of the space charge region at the interface of the ITO and p-doped PVK is reduced. As the bias across the film increases, field and space charge regions enhance hole tunneling through the interface barrier of the doped PVK film (Fig. 3(c)) [6,18], and lead to the observed current increase as compared to the undoped film.

In our experiments, we found the enhanced hole injection and transport can improve significantly the performance of OLED devices that use p-doped PVK as the HTL. Fig. 4(a) shows the current density-voltage (*J*-*V*) characteristics of the devices consisting of ITO/PVK:*x* wt.% F4-TCNQ (50 nm)/NPB (10 nm)/Alq<sub>3</sub> (60 nm)/LiF (0.5 nm)/Al (100 nm). The 10 nm NPB layer was inserted between HTL and EML to prevent the quenching of excitons at the interface between the p-doped HTL and the EML. For reference, a control device with 50 nm PVK was also fabricated under the same condition. It can be seen that the control device has

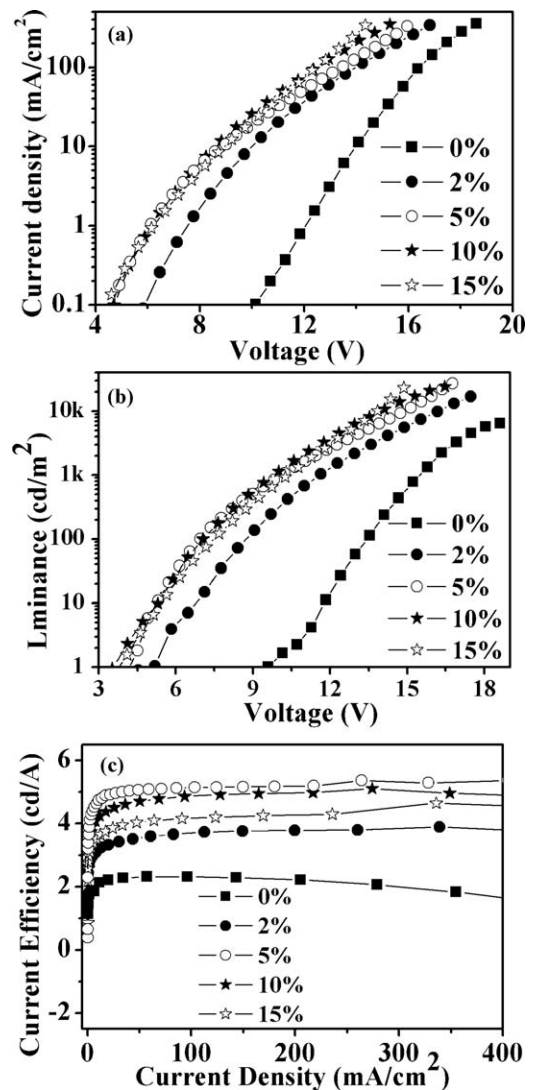


**Fig. 4.** Electric and luminescent characteristics of devices using p-doped HTLs: (a) the current density is shown as a function of voltage; (b) the luminance is shown as a function of voltage; (c) the efficiency is shown as a current density.

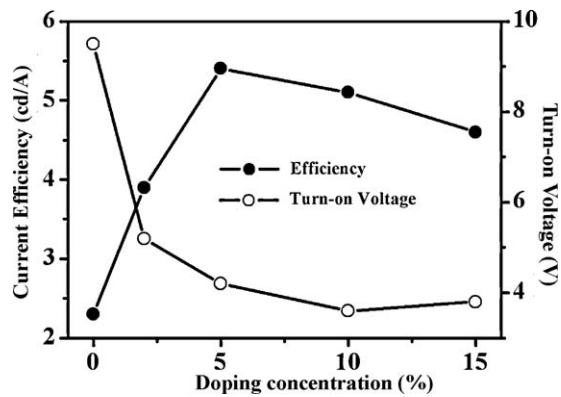


Fig. 5. The maximum current efficiency and the turn-on voltage are shown as functions of dopant concentration for all the light-emitting devices.

a high threshold voltage due to the large injection barrier. At a certain voltage, the current density increases significantly with the concentration of F4-TCNQ. This in turn reduces the device operating voltages, for example, the operating voltage decreases from 16.4 to 12.4 V at a fixed current density of 100 mA/cm<sup>2</sup> when a 15 wt.% F4-TCNQ-doped layer is used.

The luminance–voltage (*L*–*V*) characteristics of the p-doped devices are shown in Fig. 4(b). It is clear that the turn-on voltage is reduced as the concentration of F4-TCNQ is increased. For example,

the turn-on voltage (the voltage required to operate the device at a luminance intensity of 1 cd/m<sup>2</sup>) of the device with 10 wt.% F4-TCNQ doping is 3.6 V, which is reduced from 9.5 V of the control device. Similarly, the turn-on voltages of the 2, 5, and 15 wt.% doped devices are also reduced. At the concentration of 5 wt.% of F4-TCNQ, the device has the maximum brightness of 27,340 cd/m<sup>2</sup> at 16.3 V, which is 4.2 times as large as that of the control device.

We now turn to the current efficiency of the doped devices, which is also improved with the F4-TCNQ doping. From Fig. 4(c), we see that the control device has a maximum efficiency of 2.3 cd/A. However, with a doping concentration of 5 wt.%, the current efficiency reaches a maximum of 5.4 cd/A, which is enhanced by approximately 235%. We attribute these results to the decrease of the hole injection barrier and the increased conductivity in the HTL by the formation of CT complex between F4-TCNQ and PVK.

To further analyze the effects of the F4-TCNQ concentration, we show the maximum current efficiencies and turn-on voltages as a function of dopant concentration in Fig. 5 for all the devices. Fig. 5 shows that the current efficiency begins to decrease when the concentration of F4-TCNQ is above 5 wt.%. This result is likely because, when the doping concentration is more than 5 wt.%, more holes reach the NPB/Alq<sub>3</sub> interface, and create a charge imbalance at the NPB/Alq<sub>3</sub> interface, leading to the decrease of efficiency. Fig. 4 also shows the turn-on voltage as a function of the doping concentration, which has a minimal value at 10 wt.%. From these results, we believe the optimal doping concentration should be between 5 and 10 wt.%.

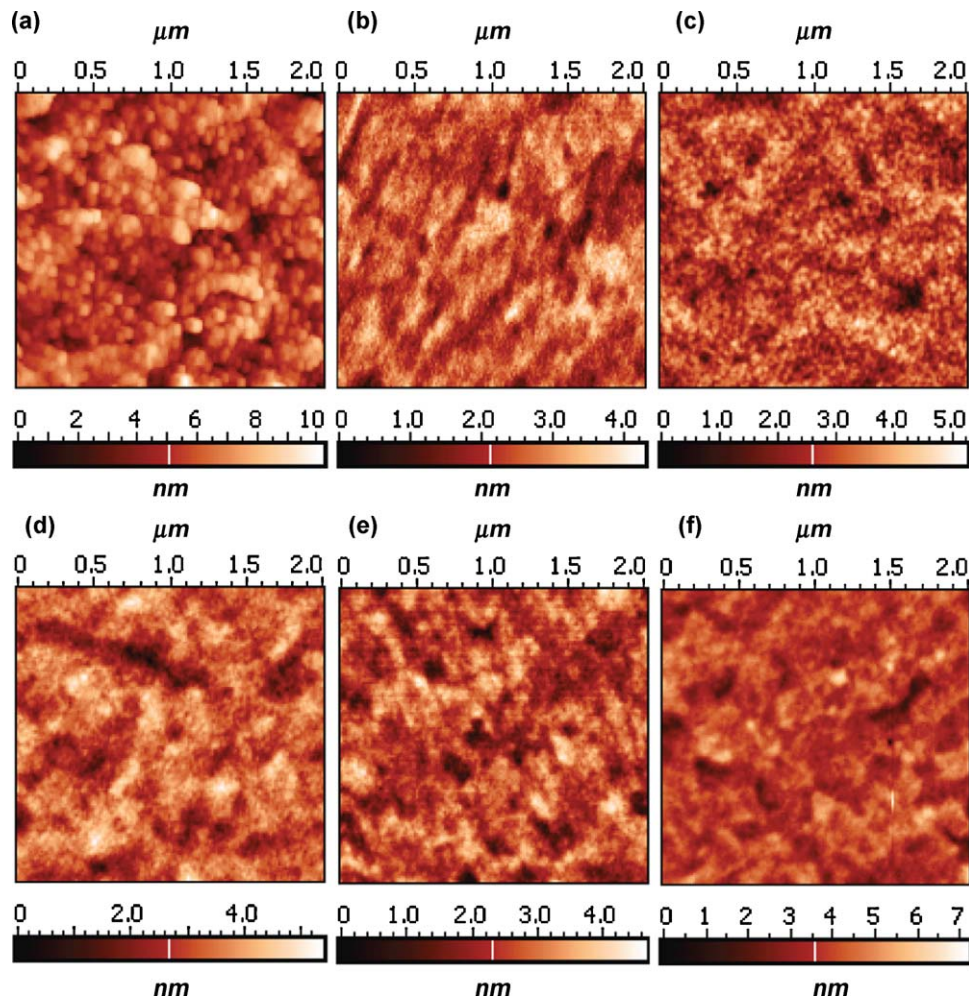


Fig. 6. AFM images (2 μm × 2 μm) of ITO substrate, PVK and p-doped PVK thin films: (a) ITO substrate, (b) PVK, (c) 2 wt.% doped PVK, (d) 5 wt.% doped PVK, (e) 10 wt.% doped PVK, and (f) 15 wt.% doped PVK. The thickness of organic films was about 50 nm.

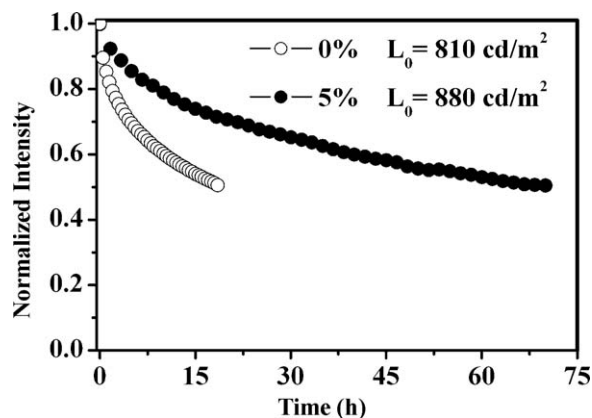


Fig. 7. Operational stabilities of the encapsulated light-emitting devices using PVK and 5 wt.% F4-TCNQ-doped PVK as the HTLs.

The surface morphology of the HTL is one of the important properties for the devices in connection with their stability [3]. Fig. 6 shows  $2\ \mu\text{m} \times 2\ \mu\text{m}$  AFM images of (a) ITO, (b) PVK, (c) 2 wt.% doped PVK, (d) 5 wt.% doped PVK, (e) 10 wt.% doped PVK, and (f) 15 wt.% doped PVK, respectively. All the organic films were spin coated on the ITO substrate and annealed for 1 h at temperature  $80\ ^\circ\text{C}$ . These experimental results show that the surface roughness of p-doped PVK film is similar to the surface of PVK, but the surfaces of organic films are quite planer than that of ITO substrate.  $R_{\text{rms}}$  (root-mean-square roughness) values were about 0.6–0.7 nm for doped PVK films and 1.3 nm for the ITO substrate. AFM observation clearly indicated that the doped PVK thin film spin coated on the ITO substrate reduced surface roughness, which is benefit for the operational stability of the devices.

We finally investigated the influence of the p-doped PVK HTL on the device stability. The lifetime of 5 wt.% F4-TCNQ-doped PVK device was measured with an initial luminance of  $880\ \text{cd}/\text{m}^2$  with a constant current density ( $17.8\ \text{mA}/\text{cm}^2$ ) operation. Similarly, the lifetime of the control device with pure PVK was measured under the condition of constant current density ( $35.7\ \text{mA}/\text{cm}^2$ ) with an initial luminance of  $810\ \text{cd}/\text{m}^2$ . As shown in Fig. 7, the half lifetime of the device with the p-doped HTL is 71.5 h, which is 3.7 times as large as that of the control device. Since it has been suggested that extra electrons can cause significant degradation of the  $\text{Alq}_3$  layer [32], the increased lifetime indicates that the increased injection and conductivity of the p-doped HTL improves the charge balance in a device.

#### 4. Conclusion

We fabricated organic light-emitting devices with F4-TCNQ-doped PVK as HTLs. Compared to the control device with undoped PVK as its HTL, the current efficiency of p-doped devices are enhanced, and the turn-on voltage is reduced significantly. At the

concentration of 5 wt.%, a maximum device brightness of  $27,340\ \text{cd}/\text{m}^2$  and a current efficiency of  $5.4\ \text{cd}/\text{A}$  are achieved. We have also found that the half lifetime of the device with 5 wt.% F4-TCNQ doped HTL is 3.7 times better than that of the control device. All these results indicate that the F4-TCNQ-doped PVK layer can significantly reduce the drive voltage, increase the current efficiency and enhance the operational stability. By analyzing doping induced effects, we have found that these enhancements can be attributed to two major causes: the enhanced hole injection and the increased hole conductivity of the p-doped HTL due to the formation of CT complex.

#### Acknowledgements

The authors are grateful to the Ministry of Science and Technology of China (program No. 2006CB921602), the Program for New Century Excellent Talents, and the Firefly Lighting Co., Ltd., in China for the financial support.

#### References

- [1] T.-Y. Chu, C.Y. Kwong, O.-K. Song, Appl. Phys. Lett. 92 (2008) 233307.
- [2] F.-C. Chen, S.-C. Chien, Y.-S. Chen, Appl. Phys. Lett. 94 (2009) 043306.
- [3] X. Zhang, Z. Wu, D. Wang, D. Wang, X. Hou, Appl. Surf. Sci. 255 (2009) 7970.
- [4] X. Zhou, J. Blochwitz, M. Pfeiffer, A. Nollau, T. Fritz, K. Leo, Adv. Funct. Mater. 11 (2001) 310.
- [5] G. Xie, Y. Meng, F. Wu, C. Tao, D. Zhang, M. Liu, Q. Xue, W. Chen, Y. Zhao, Appl. Phys. Lett. 92 (2008) 093305.
- [6] W. Gao, A. Kahn, J. Appl. Phys. 94 (2003) 359.
- [7] F. Steuber, J. Staudigel, M. Stossel, J. Simmerer, A. Winnacker, Appl. Phys. Lett. 74 (1999) 3558.
- [8] Z. Zhong, Y. Jiang, Appl. Surf. Sci. 249 (2005) 271.
- [9] J.-S. Lim, P.-K. Shin, Appl. Surf. Sci. 253 (2007) 3828.
- [10] Y. Shirota, Y. Kuwabara, H. Inada, T. Wakimoto, H. Nakada, Y. Yonemoto, S. Kawami, K. Imai, Appl. Phys. Lett. 65 (1994) 807.
- [11] T. Matsushima, Y. Kinoshita, H. Murata, Appl. Phys. Lett. 91 (2007) 253504.
- [12] J. Xu, Y. Yang, J. Yu, Y. Jiang, Appl. Surf. Sci. 255 (2009) 4329.
- [13] J.-H. Lee, D.-S. Leem, J.-J. Kim, Org. Electron. 9 (2008) 805.
- [14] C.-C. Chang, M.-T. Hsieh, J.-F. Chen, Appl. Phys. Lett. 89 (2006) 253504.
- [15] D.-S. Leem, H.-D. Park, J.-W. Kang, J.-H. Lee, J.-W. Kim, J.-J. Kim, Appl. Phys. Lett. 91 (2007) 011113.
- [16] X.L. Zhu, J.X. Sun, H.J. Peng, Z.G. Meng, M. Wong, H.S. Kwok, Appl. Phys. Lett. 87 (2005) 153508.
- [17] F. Huang, A.G. MacDiarmid, B.R. Hsieh, Appl. Phys. Lett. 71 (1997) 2415.
- [18] J. Hwang, A. Kahn, J. Appl. Phys. 97 (2005) 103705.
- [19] K.-H. Yim, G.L. Whiting, C.E. Murphy, J.J.M. Halls, J.H. Burroughes, R.H. Friend, J.-S. Kim, Adv. Mater. 20 (2008) 3319.
- [20] E.F. Aziz, A. Vollmer, S. Eisebitt, W. Eberhardt, P. Pingel, D. Neher, N. Koch, Adv. Mater. 19 (2007) 3257.
- [21] Y.-J. Yu, O. Solomeshch, H. Chechik, A.A. Goryunkov, R.F. Tuktarov, D.H. Choi, J.-I. Jin, Y. Eichen, N. Tessler, J. Appl. Phys. 104 (2008) 124505.
- [22] A. Yamamori, C. Adachi, T. Koyama, Y. Taniguchi, J. Appl. Phys. 86 (1999) 4369.
- [23] Y. Zhnag, B. de Boer, P.W.M. Blom, Adv. Funct. Mater. 19 (2009) 1901.
- [24] S. Liu, J. Shi, E.W. Forsythe, S.M. Blomquist, D. Chiu, Synth. Met. 159 (2009) 1438.
- [25] X. Jiang, Y. Liu, X. Song, D. Zhu, Synth. Met. 87 (1997) 175.
- [26] F. Michelotti, F. Borghese, M. Bertolotti, E. Cianci, V. Foglietti, Synth. Met. 111–112 (2000) 105.
- [27] M.B. Khalifa, D. Vaufrey, J. Tardy, Org. Electron. 5 (2004) 187.
- [28] Y. Shi, Z. Deng, D. Xu, Z. Chen, X. Li, Displays 28 (2007) 97.
- [29] B.J. Chen, S.Y. Liu, Synth. Met. 91 (1997) 169.
- [30] A. Kuczkowski, Eur. Polym. J. 18 (1982) 109.
- [31] G. Safoula, K. Napo, J.C. Bernède, S. Touihri, K. Alimi, Eur. Polym. J. 37 (2001) 843.
- [32] Y. Luo, H. Aziz, G. Xu, Z.D. Popovic, Chem. Mater. 19 (2007) 2079.